Outer membrane changes enable evolutionary escape from bacterial predation

Subham Mridha[1,2,§,#], Sarah-Luise Loose[1,*], Ove Ch. Mattmann[1,2,*], Saskia Isele[1], Rolf Kümmerli[2] and Simona G. Huwiler[1,#]

[1]Department of Plant and Microbial Biology, University of Zurich, Zurich, Switzerland

[2]Department of Quantitative Biomedicine, University of Zurich, Zurich, Switzerland

*** These authors contributed equally to this work**

§ Current address: Department of Microbiology, Perelman School of Medicine, University of Pennsylvania, Philadelphia, United States of America

 # Correspondence:
Subham Mridha & Simona Huwiler
subhammridha@yahoo.com & simona.huwiler@uzh.ch

Abstract

To combat antimicrobial resistant pathogens, natural predatory bacteria, like *Bdellovibrio bacteriovorus*, represent potential alternatives. *B. bacteriovorus* could be particularly potent as it kills a broad range of human bacterial pathogens, however, it remains unclear whether prey can evolve genetically-determined resistance against predation. Here, we show that the model bacterium *Escherichia coli* K-12 consistently evolves resistance against *B. bacteriovorus* during experimental evolution. Selection for resistance scaled positively with predation pressure and was widespread after two cycles of predator exposure. Like antibiotics, predation resistance was costly, manifesting in a trade-off between predation resistance and fitness in the absence of predators. Genetic analysis identified changes in outer membrane porin OmpF as common resistance mechanism, while a mutation in cell envelope lipopolysaccharide-modifying enzyme WaaF was rarer but also conferred predation resistance. Our study uncovers evolutionary and mechanistic aspects of prey escape from predation, generating important knowledge on predator-prey interactions and to advance sustainable treatments.

Keywords: predator-prey interaction, predatory bacteria, *Escherichia coli*, *Bdellovibrio bacteriovorus*, predation resistance, evolution, prey escape

Introduction

Bacterial resistance to conventional antibiotics is a major public health concern, that led to 1.27 million deaths in 2019[1]. This urgently calls for the discovery of novel antibiotics and alternative treatment strategies[2–4]. One promising alternative involves the use of natural bacterial predators including bacteriophages (viruses of bacteria)[5] and predatory bacteria[3,6], which are environmentally widespread[7]. While phage therapy is currently extensively studied[2], much less is known about the potential of predatory bacteria, like *Bdellovibrio bacteriovorus*, that kill and invade pathogenic bacteria and are therefore considered 'living antibiotics'[3,6]. *B. bacteriovorus* is capable of killing growing and stationary phase bacterial prey cells, and in addition irrespective of their antibiotic resistance[8–10].

Similar to bacteriophages, *B. bacteriovorus* is neither toxic nor pathogenic to eukaryotic cells and is therefore of great promise[3,6]. However, key differences exist between the two predator types. For example, bacteriophages are typically very specific to prey strains, whereas *B. bacteriovorus* is a generalist with a broad prey range[11,12]. This makes *B. bacteriovorus* suitable to treat polymicrobial infections[11,13]. Moreover, there seem to be few defence and immunity mechanisms present among prey species to defend themselves against *B. bacteriovorus*[14,15]. This contrasts with the over hundred specific bacterial defence and immune systems reported against bacteriophages[16]. Thus, *B. bacteriovorus* might be a more effective treatment under certain circumstances, compared to traditional antibiotics and bacteriophages.

Despite these promising aspects, little is known on the selection pressures that *B. bacteriovorus* may impose on its prey and the evolutionary responses it may trigger[17–19]. Some evolutionary studies, focussing on predator-prey interactions, reported evidence for resistance evolution[17–19] but did not explore the underlying mechanisms on a phenotypic and genotypic level. While recognition of the prey and prey invasion is likely multifactorial[20,21], potentially hindering fast resistance formation, prey resistance has been described transient[3,22]. One study described a form of phenotypic (plastic) resistance, whereby several prey species developed a transient yet reversible stage of predation resilience[22]. Finally, several studies highlighted that secretion systems[23] and secreted compounds such as quorum-sensing signals[24,25], indole[26] and cyanide[27] may offer some protection from *B. bacterivorous* predation, while the presence of paracrystalline protein surface (S-) layers seems to prevent killing in certain bacterial species[14].

To obtain a systematic and in-depth understanding of the potential of prey to evolve resistance to *B. bacteriovorus*, we performed an experimental prey evolution study with the model organism *E. coli* K-12 as prey and *B. bacteriovorus* HD100 as predator. Upon repeated and intermittent exposure of prey to different predator concentrations, we found strong evidence that *E. coli* K-12 predominantly evolves genetically-based predation resistance under high predatory pressure, whereas increased growth due to media adaptation and phenotypic effects played minor roles. Evolutionary escape from predation evolved repeatedly across independently evolved prey lineages. Predation resistance is costly and manifested in a negative association between the resistance level of a lineage and its growth in the absence of predation. A combination of population sequencing with high genome coverage and single-gene deletion mutant experiments revealed that mutations in the outer membrane porin OmpF, and an enzyme (WaaF) involved in lipopolysaccharide (LPS) modification are involved with resistant phenotypes. These results suggest that the prey modifies different potential points of contact with the predator[15,20]. Our study elucidates the ecological context, the evolutionary path, and the molecular mechanisms of prey resistance evolution against *B. bacteriovorus*, generating key knowledge for the development of bacterial predators as sustainable 'living antibiotics'.

Results

Experimental evolution leads to increased prey growth

We experimentally evolved *E. coli* K-12 prey under no, low and high predatory pressures of *B. bacteriovorus* HD100 in eightfold replication. Experimental prey evolution was conducted for 15 alternate cycles of predation and prey recovery (Fig. 1a, Extended Data Fig. 1). After prey evolution, we subjected all evolved prey lineages to the predation pressure they experienced during experimental evolution. We found significant growth differences across the three predatory pressures (ANOVA: $F_{2,141} = 8780.2$, $p < 0.0001$). All *E. coli* lineages evolved without predator grew significantly better than the ancestor (red dotted line), which indicates media adaptation (Fig. 1b+e). For prey lineages evolved with predators, we observed that five low-predator evolved lineages (L1-L5, Fig. 1c+f) and all high-predator evolved lineages (H1-H8, Fig. 1d+g) showed significant growth recovery relative to the ancestor subjected to predation (black dotted line). For most of these lineages (84.6%), growth recovery was partial, while only two lineages (H4, H5, 15.4%) showed complete recovery, compared to the unchallenged ancestor. Moreover, growth under predation was higher for prey lineages evolved

80 under high than under low predatory pressure. Altogether, these results suggest that prey evolved
81 partial resistance to predation and that higher predation pressure selected for higher levels of resistance.

82

83 **Predation and not media adaptation drives resistance evolution**

84 Media adaptation could be a simple explanation for the observed resistance phenotypes because faster
85 growth would allow the prey to outpace the predator's killing speed. If this hypothesis holds true we
86 expect that no-predator evolved lineages, which showed highly improved growth, should be able to
87 resist predation. We found no support for this hypothesis as all no-predator evolved lineages were still
88 fully susceptible to predation (Fig. 2a, c). Instead, our results show that lineages L1-L5 (which evolved
89 partial resistance under low predation) were also able to grow under high predatory pressure (Fig. 2b,
90 d). We even observed slightly increased growth in a previously unnoticed lineage (L8). Together, these
91 results indicate that adaptations are predation-specific and not driven by media adaptation.

92

93 **Predation resistance arises early and remains persistent over time**

94 Next, we examined the temporal pattern of predation resistance evolution. We noticed that prey optical
95 density (OD_{600nm}) already increased at the second evolution cycle and fluctuated at a relatively high
96 level thereafter (Extended Data Fig. 1a). To verify that resistance arose early, we repeated the growth
97 experiments shown in Fig. 1b-g with all high-predator lineages (H1-H8) from the 2nd and 5th evolution
98 cycle (Extended Data Fig. 1 and 2). These analyses confirmed that predation-resistant phenotypes
99 emerged early on during experimental evolution as all lineages could readily grow under high predation
100 pressure at evolution cycle 2, with barely any growth differences existing compared to later evolution
101 cycles 5 and 15 (Extended Data Fig. 1 and 2). Hence, predation resistance evolved early and once
102 emerged within a prey lineage it remained persistent over generations.

103

104 **Trade-off between predation resistance and prey growth in the absence of predation**

105 Antibiotics resistance is often associated with fitness costs in the absence of antibiotics[28,29]. Here, we
106 tested whether a similar trade-off occurs for *E. coli* in the context of predation resistance. To investigate

107 this, we grew all evolved lineages without predators and calculated their growth rate relative to the
108 ancestor. Relative growth rates differed significantly across predatory pressures (ANOVA: $F_{2,141}$ =
109 460.42, $p < 0.0001$), and were highest in no-predator evolved *E. coli* lineages (Fig. 3a, d), followed by
110 low-predator evolved lineages with growth rates similar to the ancestor (Fig. 3b, e) and high-predator
111 evolved lineages with generally lower growth rate than the ancestor (Fig. 3c, f). When contrasting these
112 growth rates against relative prey resistance (quantified as relative growth integral under high predatory
113 pressure), we found a significant negative correlation between predation resistance and prey fitness,
114 indicating the predicted trade-off (Fig. 3g). Thus, our findings corroborate that *E. coli* resistance
115 mechanisms are costly in the absence of *B. bacteriovorus* predation.

116

117 **High consistency in resistance levels among single clones**

118 Based on the detected trade-off between predation resistance and population prey growth, we wondered
119 whether there is heterogeneity in predation resistance among clones within prey populations.
120 Consequently, we analysed the predation resistance profile of six randomly isolated clones from each
121 of the eight high-predator lineages (15th cycle, 48 clones) and found that all clones showed consistently
122 high predation resistance. This shows that clones did not separate into susceptible and resistant
123 phenotypes (Extended Data Fig. 4 and 5) and thus did not segregate along a trade-off line within
124 populations. This result further indicates that the mechanisms conferring resistance to predation likely
125 operate at the individual and not at the group level of the prey. Such group-level mechanisms were
126 proposed to operate via the secretion of small soluble substances (quorum-sensing signals, indole,
127 cyanide)[24–27] and are expected to protect not only the evolved producers but also susceptible wildtype
128 cells.

129

130 **Mutation frequency in the prey genome peaks under high predatory pressure**

131 To uncover the genetic basis of putative resistance mechanisms, we sequenced all 24 evolved *E. coli*
132 lineages (N1-8: no predation, L1-8: low predation, H1-8: high predation) after the 15th evolution cycle
133 along with the original ancestor with high sequencing depth. The Illumina sequencing reads were
134 mapped to the reference genome of *E. coli* K-12 MG1655 and multi-sample variant calling with a
135 frequency cutoff of 5% was performed. We focused on *E. coli* genes that had mutations in evolved

136 lineages but not in the ancestor (Extended Data Fig. 6). We excluded mutated rRNA and transposase
137 genes because they did not correlate with any of the three evolution conditions (Extended Data Fig. 7).
138 Using these filters, we uncovered 43 mutated genes of which 17 occurred in N-lineages, 17 in L-
139 lineages and 30 in H-lineages (Fig. 4a). A total of 26 genes mutated exclusively under predatory
140 pressure (Fig. 4a), and thus reflect the top candidates potentially explaining resistance phenotypes. H-
141 lineages, had more exclusive gene mutations than L-lineages (18 vs. 5, Fig. 4b). Moreover, there were
142 fewer high-frequency mutations (>70%) among L-lineages than among H-lineages (Fig. 4b), which is
143 likely explained by the higher selection pressure.

144

145 **Outer membrane porin OmpF mutations repeatedly arose and confer resistance to predation**

146 Next, we conducted a cluster analysis (Fig. 4b) and analyzed the functions of the mutated gene products
147 including mutation types and (predicted) amino acid changes (Fig. 4c, Extended Data Table 1). These
148 analyses yielded *ompF*, encoding the outer membrane porin F, as the most frequently mutated gene.
149 Four H-lineages (H2, H4, H6 & H7) and two L-lineages (L1, L2) had mutations in this gene. Moreover,
150 lineage H3 had a point mutation in the upstream region of *ompF* (Extended Data Fig. 8) and lineage
151 H8 had an inframe insertion in *envZ* (Extended Data Table 1), which encodes a sensor histidine kinase
152 involved in OmpF regulation[30]. Mutation frequencies were high (73.6%-100%) in all lineages except
153 in L2. The sequencing of six individual clones per H-lineage showed that mutations in *ompF* and *envZ*
154 were present in all clones (Extended Data Fig. 9). Overall, there were no major differences in
155 mutational patterns between clonal and population level sequencing (Extended Data Fig. 9), reinforcing
156 the view of selective sweeps of a few beneficial mutations through populations. Mutation types in
157 *ompF* include missense variants (H2), frameshifts (H4, H6, H7) and direct stop gains (L1, L2) (Fig.
158 4b, c, Extended Data Fig. 8, Extended Data Table 1), indicating that most observed mutations probably
159 lead to OmpF function loss.

160 To directly test whether the loss of OmpF (a known attachment side for phages and known to be critical
161 for effective *B. bacteriovorus* predation[15]) confers resistance to predation, we generated a clean, single
162 deletion Δ*ompF* mutant based on the *E. coli* KEIO library (details in methods, Supplementary Online
163 material Table SOnline1). First, we confirmed that *E. coli* KEIO reference strain (BW25113) was fully
164 susceptible to *B. bacteriovorus* and grew well in the absence of predation (Fig. 5a,b), thus showing
165 similar responses as the *E. coli* K-12 ancestor (Fig. 1b,d and 2a,b). We then subjected the Δ*ompF*

166 mutant to no and high predation pressures and tracked its growth. We found this mutant to be
167 completely resistant to predation, showing full growth recovery under high predator exposure (Fig.
168 5a,b). We repeated the above experiments with a Δ*envZ* clean deletion mutant and found that this
169 mutant was still susceptible to predation, in agreement with Mun et al.[15] (Fig. 5a, b). This is
170 unsurprising because the experimentally evolved *envZ* mutant involved an inframe insertion [insertion
171 of Lys-Thr-Trp-Leu between Leu135 and Lys136] and not a deletion. We suspect that the insertional
172 mutation in our experiment might upregulate OmpR, resulting in lower levels of OmpF. We thus
173 conclude that functional changes in EnvZ, but not loss-of-function, could confer predation resistance.
174 In summary, our results indicate that predation resistance is primarily driven by OmpF loss-of-function
175 mutations.

176

177 **Mutations in *truA* cause costly prey morphology change**

178 In lineage H8, a high frequency mutation occurred in *truA* (100%, missense: Val200Ala) in addition
179 to the above-described *envZ* mutation (77.5%). The *truA* gene encodes the tRNA pseudouridine
180 synthase A important for protein synthesis[31]. Phase-contrast microscopy revealed that cells from
181 lineage H8 no longer separated properly after cell division resulting in cells being thinner and longer
182 (Extended Data Fig. 3a-c). Experiments with a Δ*truA* clean deletion mutant confirmed division
183 abnormalities (Extended Data Fig. 3), matching previously reported results on the effect of *truA*
184 disruption[32]. No such abnormalities in cell morphology occurred in the other H- and L-lineages
185 (Extended Data Fig. 3, Fig. SOnline1). However, deletion of *truA* did not result in predation resistance
186 but was rather associated with severe fitness costs in the absence of predation (Fig. 5). We hypothesise
187 that the resistance phenotype observed in the evolved *truA* mutant is masked in the clean deletion
188 mutant due the detrimental effects on cell division (Fig. 5). Further, our mutation frequency data
189 suggest that the missense mutation in *truA* (100%) happened first and was associated with a drop in
190 final OD_{600nm} after the recovery phase of early evolution cycles 1-5. Growth only recovered in later
191 cycles, likely due to the additional mutation in *envZ* (77.5%), probably partly compensating the fitness
192 drop (Extended Data Fig. 1b). Altogether, our results indicate that resistance to predation may occur
193 through cell morphology changes. However, such events might be rare due to the severe fitness costs
194 typically associated with changes in fundamental cell physiological processes.

195

196 **Mutation in LPS synthesis gene *waaF* confers partial resistance to predation**

197 In lineage H5, a high frequency mutation occurred in *waaF* (100%, missense: Ala255Glu), encoding
198 an heptosyltransferase involved in the biosynthesis of the lipopolysaccharide (LPS) inner core[33]. We
199 hypothesized that modification or abolishment of outer membrane structures could represent a
200 mechanism through which *E coli* can become resistant to predation. In support of our hypothesis, we
201 found that a Δ*waaF* clean deletion mutant showed partial and significant resistance to predation (Fig.
202 5a,b). The same hypothesis could also hold true for the high frequency mutation observed in *waaB*
203 (lineage H4, 87.5%, stop codon gained) encoding a galactosyltransferase involved in LPS biosynthesis.
204 However, contrary to our expectation we did not find Δ*waaB* (clean deletion mutation) to be resistant
205 to predation (Fig. 5a,b). Instead, it showed significant growth improvements in the absence of predation
206 (Fig. 5c,d). Because the mutation in *waaB* occurred together with an *ompF* mutation in lineage H4 we
207 conclude that WaaB loss-of-function does not confer predation resistance but is beneficial in an already
208 resistant lineage, showing the highest growth recovery under predation among all H-lineages (Fig. 1g).

209

210 # Discussion

211 Historical records on antibiotics tell us that bacterial pathogens have evolved resistance to every single
212 drug used in clinics. Nowadays, it is therefore imperative to understand putative mechanisms and paths
213 to resistance already during the development of new antibacterials[34,35]. In our study, we performed this
214 task for the predatory bacterium *B. bacteriovorus*, which is regarded as a potential 'living antibiotic'
215 preying on human pathogens. We found that the model prey *E. coli* K-12 MG1655 consistently evolved
216 resistance against predation through two main mechanisms: change in the outer membrane porin OmpF
217 (several independent events), and change in WaaF (one event), an enzyme involved in outer membrane
218 LPS biosynthesis. These mechanisms suggest that selection acts on cell-membrane associated traits
219 that form the first line of contact between prey and predators. The uncovered resistance mechanisms
220 are similar to the ones observed to evolve against bacteriophages[36,37] (loss/alteration of host
221 receptors[38,39]) and against membrane-targeting polymyxin antibiotics (LPS modifications)[40].

222 OmpF enables *E. coli* to import and export small molecules via passive diffusion. Osmolarity of the
223 environment likely effects prey susceptibility towards *B. bacteriovous*. It is known that *E. coli*
224 expresses high levels of OmpF under neutral pH, whereas high osmolarity leads to its
225 downregulation[41]. OmpF serves as an entry point for bacterial toxins (colicin) and antibiotics[42–44] while

226 simultaneously serving as docking site for certain bacteriophages[38,39]. However, its role in the
227 interaction with *B. bacteriovorus* is not yet resolved, apart from the fact that the deletion of OmpF
228 slows predation rate[15] and that mutations in this gene are under selection in response to predation in
229 our study. We can thus only speculate about how loss or impairment of OmpF could foster predation
230 resistance, and we propose three scenarios. Firstly, change of OmpF could prevent predators to use the
231 porin as a docking site for attachment[15], similar to phage invasion[38,39]. Secondly, OmpF might serve as
232 an 'overpressure valve' equilibrating the osmotic pressure building up when *B. bacteriovorus* enters
233 the prey periplasm. Loss of OmpF or a reduction in its small molecule transport rate might compromise
234 this function and presumably slow down predator entry. Thirdly, loss of OmpF could reduce the entry
235 of potential, hypothetical small molecules secreted by the predator. Such molecules could manipulate
236 the prey during attachment and recent evidence indicates that *B. bacteriovorus* can kill the prey even
237 without subsequent entry[45]. Altogether, our results combined with previous reports indicate that OmpF
238 is a mutational hotspot in the context of resistance evolution against antibiotics, bacteriophages, and
239 predatory *B. bacteriovorus*.

240 Important to note is that the relevance of OmpF for successful *B. bacteriovorus* predation seems to
241 depend on the prey species[15]. For example, deletion of OmpF in *Salmonella enterica* did not reduce
242 prey killing[15]. Instead, it was reported that the LPS core has a major influence on attachment[46,47]. This
243 finding combined with our results (showing that mutations in LPS-modifying enzymes WaaF and
244 WaaB were under selection) strongly support the view that LPS structure takes on an important role in
245 the interactions with predators. Work with bacteriophages revealed two opposite roles for LPS
246 (particularly the long O-antigens): depending on their specific structure they may act as primary
247 receptors for attachment or block attachment to the outer membrane[38,39]. Several lines of evidence
248 suggest that the dual role also applies to interactions with *B. bacteriovorus*[20,46,48]. First, a phage-tail
249 fiber protein homolog of *B. bacteriovorus* was indeed shown to bind to multiple bacterial surface
250 glycans/LPS in multiple prey species (*E. coli* K-235, *Serratia marcescens* and *Proteus mirabilis*)[20].
251 Second, attachment to prey is slowed down when predators are confronted with complex O-antigens
252 as opposed to shorter LPS only featuring the core oligosaccharides in several species (*S. enterica*,
253 *E. coli*, *Vibrio cholerae*)[46 48]. In sum, our results indicate that evolutionary change in LPS structure can
254 modulate prey-predator interactions as observed for bacteriophage-bacteria interactions.

255 At first sight, our results on repeated resistance evolution seem to dampen the hope for predatory
256 bacteria to become sustainable antibacterial treatments. Nonetheless, our experiments also revealed

257 good news. Particularly, the strong fitness trade-off between resistance to predation and growth in the
258 absence of predation highlights that genetically manifested predation resistance is costly,
259 compromising cellular functionality. This phenomenon could limit the spread of resistant prey as they
260 are weak competitors and probably cleared away more efficiently by macrophages. There are concepts
261 to leverage such competitive constraints to increase treatment sustainability[28,49]. A key condition for
262 leveraging on competitive constraints is that the pathogen is eliminated before compensatory mutations
263 arise. We observed two putative compensatory mutations in our experiments (mutation in *waaB* in the
264 background of an *ompF* mutant; mutation in *envZ* in the background of a *truA* mutant). Clearly, more
265 research is required to understand the propensity of resistant prey mutants (with and without
266 compensatory mutations) to spread. Moreover, it will be important to test whether similar evolutionary
267 patterns (type of mutants, compensatory mutants and speed of resistance development) are detected
268 when using predatory *B. bacteriovorus* against pathogenic bacteria and clinical isolates as prey to
269 assess the sustainability of this 'living antibiotic'.

270 To conclude, we like to emphasize two important points regarding prey resistance against bacterial
271 predation by *B. bacteriovorus*. First, resistance mechanisms do not need to offer complete protection
272 to escape predation. Instead, it suffices to alter the balance between prey growth and killing rate. In our
273 experiment, we detected a decrease in killing rate (by mutations in *ompF* and *waaF*), but no increase
274 in prey growth rate. Second, while we focused on predation resistance through mutation and selection
275 processes, previous work has reported 'plastic' resistance phenotypes, occurring after short timescale
276 exposures, offering transiently protection against *B. bacteriovorus*[22]. Such plastic effects also surface
277 in response to colistin exposure (i.e. change in membrane polarity) and might well have occurred in
278 our experiments (e.g., in resistant prey lineages exposed to low predatory pressure with few low
279 frequency genetic mutations). A key task for future studies is to integrate all these aspects and to
280 understand the dynamics of prey resistance and predation escape under situations that are closer to
281 clinical settings – for example using clinical pathogen isolates, assessing treatment efficacy in spatially
282 structured human cell cultures, and allowing predators to co-evolve with the prey. Only with such
283 integrative knowledge, we can ensure the long-term sustainability of *B. bacteriovorus* as a 'living
284 antibiotic', efficient in targeting multi-drug resistant pathogens, in clinically relevant contexts.

285

286 # References (Main text)

287 1. Murray, C. J., et al. Global burden of bacterial antimicrobial resistance in 2019: a systematic
288 analysis. *The Lancet* **399,** 629–655 (2022).

289 2. Pirnay, J.-P., et al. Personalized bacteriophage therapy outcomes for 100 consecutive cases: a
290 multicentre, multinational, retrospective observational study. *Nat Microbiol* **9,** 1434–1453
291 (2024).

292 3. Sockett, R. E. & Lambert, C. Bdellovibrio as therapeutic agents: a predatory renaissance? *Nat*
293 *Rev Microbiol* **2,** 669–675 (2004).

294 4. Konwar, A. N., Hazarika, S. N., Bharadwaj, P. & Thakur, D. Emerging Non-Traditional
295 Approaches to Combat Antibiotic Resistance. *Curr Microbiol* **79,** 330 (2022).

296 5. Koskella, B., Hernandez, C. A. & Wheatley, R. M. Understanding the Impacts of
297 Bacteriophage Viruses: From Laboratory Evolution to Natural Ecosystems. *Annu. Rev. Virol.* **9,**
298 57–78 (2022).

299 6. Atterbury, R. J. & Tyson, J. Predatory bacteria as living antibiotics - where are we now?
300 *Microbiology (Reading)* **167,** (2021).

301 7. Lai, T. F., Ford, R. M. & Huwiler, S. G. Advances in cellular and molecular predatory biology
302 of *Bdellovibrio bacteriovorus* six decades after discovery. *Front. Microbiol.* **14,** 1168709
303 (2023).

304 8. Saralegui, C., Herencias, C., Halperin, A. V., De Dios-Caballero, J., Pérez-Viso, B., Salgado,
305 S., Lanza, V. F., Cantón, R., Baquero, F., Prieto, M. A. & Del Campo, R. Strain-specific
306 predation of *Bdellovibrio bacteriovorus* on *Pseudomonas aeruginosa* with a higher range for
307 cystic fibrosis than for bacteremia isolates. *Sci Rep* **12,** 10523 (2022).

308 9. Upatissa, S., Mun, W. & Mitchell, R. J. Pairing Colicins B and E5 with *Bdellovibrio*
309 *bacteriovorus* To Eradicate Carbapenem- and Colistin-Resistant Strains of *Escherichia coli*.
310 *Microbiol Spectr* **11,** e00173-23 (2023).

311 10. Sun, Y., Ye, J., Hou, Y., Chen, H., Cao, J. & Zhou, T. Predation Efficacy of *Bdellovibrio*
312 *bacteriovorus* on Multidrug-Resistant Clinical Pathogens and Their Corresponding Biofilms.
313 *Jpn J Infect Dis* **70,** 485–489 (2017).

314 11. Dashiff, A., Junka, R. A., Libera, M. & Kadouri, D. E. Predation of human pathogens by the
315 predatory bacteria *Micavibrio aeruginosavorus* and *Bdellovibrio bacteriovorus*: Predation by
316 *M. aeruginosavorus* and *B. bacteriovorus*. *Journal of Applied Microbiology* **110,** 431–444
317 (2011).

318 12. Jurkevitch, E., Minz, D., Ramati, B. & Barel, G. Prey Range Characterization, Ribotyping, and
319 Diversity of Soil and Rhizosphere *Bdellovibrio* spp. Isolated on Phytopathogenic Bacteria. *Appl*
320 *Environ Microbiol* **66,** 2365–2371 (2000).

321 13. Im, H., Choi, S. Y., Son, S. & Mitchell, R. J. Combined Application of Bacterial Predation and
322 Violacein to Kill Polymicrobial Pathogenic Communities. *Sci Rep* **7,** 14415 (2017).

323 14. Koval, S. F. & Hynes, S. H. Effect of paracrystalline protein surface layers on predation by
324 *Bdellovibrio bacteriovorus*. *J Bacteriol* **173,** 2244–2249 (1991).

325 15. Mun, W., Upatissa, S., Lim, S., Dwidar, M. & Mitchell, R. J. Outer Membrane Porin F in *E.*
326 *coli* Is Critical for Effective Predation by *Bdellovibrio*. *Microbiol Spectr* **10,** e03094-22 (2022).

327 16. Georjon, H. & Bernheim, A. The highly diverse antiphage defence systems of bacteria. *Nat Rev*
328 *Microbiol* **21,** 686–700 (2023).

329 17. Varon, M. Selection of predation-resistant bacteria in continuous culture. *Nature* **277,** 386–388
330 (1979).

331 18. Gallet, R., Alizon, S., Comte, P.-A., Gutierrez, A., Depaulis, F., van Baalen, M., Michel, E. &
332 Muller-Graf, C. D. M. Predation and Disturbance Interact to Shape Prey Species Diversity.
333 **170,** 143–154 (2007).

334 19. Gallet, R., Tully, T. & Evans, M. E. K. Ecological conditions affect evolutionary trajecory in a
335 predator-prey system. *Evolution* **63,** 641–651 (2009).

336 20. Caulton, S. G., Lambert, C., Tyson, J., Radford, P., Al-Bayati, A., Greenwood, S., Banks, E. J.,
337 Clark, C., Till, R., Pires, E., Sockett, R. E. & Lovering, A. L. *Bdellovibrio bacteriovorus* uses

338 chimeric fibre proteins to recognize and invade a broad range of bacterial hosts. *Nat Microbiol*
339 **9,** 214–227 (2024).

340 21. Chanyi, R. M., Ward, C., Pechey, A. & Koval, S. F. To invade or not to invade: two
341 approaches to a prokaryotic predatory life cycle. *Can J Microbiol* **59,** 273–279 (2013).

342 22. Shemesh, Y. & Jurkevitch, E. Plastic phenotypic resistance to predation by *Bdellovibrio* and
343 like organisms in bacterial prey. *Environmental Microbiology* **6,** 12–18 (2004).

344 23. Aharon, E., Mookherjee, A., Pérez-Montaño, F., Mateus Da Silva, G., Sathyamoorthy, R.,
345 Burdman, S. & Jurkevitch, E. Secretion systems play a critical role in resistance to predation by
346 *Bdellovibrio bacteriovorus*. *Research in Microbiology* **172,** 103878 (2021).

347 24. Hoshiko, Y., Nishiyama, Y., Moriya, T., Kadokami, K., López-Jácome, L. E., Hirano, R.,
348 García-Contreras, R. & Maeda, T. Quinolone Signals Related to Pseudomonas Quinolone
349 Signal-Quorum Sensing Inhibits the Predatory Activity of *Bdellovibrio bacteriovorus*. *Front.*
350 *Microbiol.* **12,** 722579 (2021).

351 25. Dwidar, M., Jang, H., Sangwan, N., Mun, W., Im, H., Yoon, S., Choi, S., Nam, D. & Mitchell,
352 R. J. Diffusible Signaling Factor, a Quorum-Sensing Molecule, Interferes with and Is Toxic
353 Towards *Bdellovibrio bacteriovorus* 109J. *Microb Ecol* **81,** 347–356 (2021).

354 26. Dwidar, M., Nam, D. & Mitchell, R. J. Indole negatively impacts predation by *B dellovibrio*
355 *bacteriovorus* and its release from the bdelloplast. *Environmental Microbiology* **17,** 1009–1022
356 (2015).

357 27. Mun, W., Kwon, H., Im, H., Choi, S. Y., Monnappa, A. K. & Mitchell, R. J. Cyanide
358 Production by *Chromobacterium piscinae* Shields It from *Bdellovibrio bacteriovorus* HD100
359 Predation. *mBio* **8,** e01370-17 (2017).

360 28. Andersson, D. I. & Hughes, D. Antibiotic resistance and its cost: is it possible to reverse
361 resistance? *Nat Rev Microbiol* **8,** 260–271 (2010).

362 29. Andersson, D. I. The biological cost of mutational antibiotic resistance: any practical
363 conclusions? *Current Opinion in Microbiology* **9,** 461–465 (2006).

364 30. Cai, S. J. & Inouye, M. EnvZ-OmpR Interaction and Osmoregulation in *Escherichia coli.*
365 *Journal of Biological Chemistry* **277,** 24155–24161 (2002).

366 31. Davis, D. R. & Poulter, C. D. Proton-nitrogen-15 NMR studies of *Escherichia coli* tRNAPhe
367 from HisT mutants: a structural role for pseudouridine. *Biochemistry* **30,** 4223–4231 (1991).

368 32. Tsui, H. C., Arps, P. J., Connolly, D. M. & Winkler, M. E. Absence of hisT-mediated tRNA
369 pseudouridylation results in a uracil requirement that interferes with *Escherichia coli* K-12 cell
370 division. *J Bacteriol* **173,** 7395–7400 (1991).

371 33. Gronow, S., Brabetz, W. & Brade, H. Comparative functional characterization *in vitro* of
372 heptosyltransferase I (WaaC) and II (WaaF) from *Escherichia coli*. *European Journal of*
373 *Biochemistry* **267,** 6602–6611 (2000).

374 34. Aminov, R. I. A Brief History of the Antibiotic Era: Lessons Learned and Challenges for the
375 Future. *Front. Microbio.* **1,** (2010).

376 35. Davies, J. & Davies, D. Origins and Evolution of Antibiotic Resistance. *Microbiol Mol Biol*
377 *Rev* **74,** 417–433 (2010).

378 36. Fang, Q., Feng, Y., McNally, A. & Zong, Z. Characterization of phage resistance and phages
379 capable of intestinal decolonization of carbapenem-resistant *Klebsiella pneumoniae* in mice.
380 *Commun Biol* **5,** 48 (2022).

381 37. Oechslin, F. Resistance Development to Bacteriophages Occurring during Bacteriophage
382 Therapy. *Viruses* **10,** 351 (2018).

383 38. Maffei, E., Shaidullina, A., Burkolter, M., Heyer, Y., Estermann, F., Druelle, V., Sauer, P.,
384 Willi, L., Michaelis, S., Hilbi, H., Thaler, D. S. & Harms, A. Systematic exploration of
385 *Escherichia coli* phage–host interactions with the BASEL phage collection. *PLoS Biol* **19,**
386 e3001424 (2021).

387 39. Nobrega, F. L., Vlot, M., De Jonge, P. A., Dreesens, L. L., Beaumont, H. J. E., Lavigne, R.,
388 Dutilh, B. E. & Brouns, S. J. J. Targeting mechanisms of tailed bacteriophages. *Nat Rev*
389 *Microbiol* **16,** 760–773 (2018).

390 40. Jochumsen, N., Marvig, R. L., Damkiær, S., Jensen, R. L., Paulander, W., Molin, S., Jelsbak, L.
391 & Folkesson, A. The evolution of antimicrobial peptide resistance in *Pseudomonas aeruginosa*
392 is shaped by strong epistatic interactions. *Nat Commun* **7,** 13002 (2016).

393 41. Kenney, L. J. & Anand, G. S. EnvZ/OmpR Two-Component Signaling: An Archetype System
394 That Can Function Noncanonically. *EcoSal Plus* **9,** 10.1128/ecosalplus.ESP-0001–2019 (2020).

395 42. Thanassi, D. G., Suh, G. S. & Nikaido, H. Role of outer membrane barrier in efflux-mediated
396 tetracycline resistance of *Escherichia coli*. *J Bacteriol* **177,** 998–1007 (1995).

397 43. Choi, U. & Lee, C.-R. Distinct Roles of Outer Membrane Porins in Antibiotic Resistance and
398 Membrane Integrity in *Escherichia coli*. *Front. Microbiol.* **10,** 953 (2019).

399 44. Delcour, A. H. Outer membrane permeability and antibiotic resistance. *Biochimica et*
400 *Biophysica Acta (BBA) - Proteins and Proteomics* **1794,** 808–816 (2009).

401 45. Tyson, J., Radford, P., Lambert, C., Till, R., Huwiler, S. G., Lovering, A. L. & Elizabeth
402 Sockett, R. Prey killing without invasion by *Bdellovibrio bacteriovorus* defective for a
403 MIDAS-family adhesin. *Nat Commun* **15,** 3078 (2024).

404 46. Varon, M. & Shilo, M. Attachment of *Bdellovibrio bacteriovorus* to cell wall mutants of
405 *Salmonella* spp. and *Escherichia coli*. *J Bacteriol* **97,** 977–979 (1969).

406 47. Schelling, M. & Conti, S. Host receptor sites involved in the attachment of *Bdellovibrio*
407 *bacteriovorus* and *Bdellovibrio stolpii*. *FEMS Microbiology Letters* **36,** 319–323 (1986).

408 48. Duncan, M. C., Forbes, J. C., Nguyen, Y., Shull, L. M., Gillette, R. K., Lazinski, D. W., Ali,
409 A., Shanks, R. M. Q., Kadouri, D. E. & Camilli, A. *Vibrio cholerae* motility exerts drag force
410 to impede attack by the bacterial predator *Bdellovibrio bacteriovorus*. *Nat Commun* **9,** 4757
411 (2018).

412 49. Wale, N., Sim, D. G., Jones, M. J., Salathe, R., Day, T. & Read, A. F. Resource limitation
413 prevents the emergence of drug resistance by intensifying within-host competition. *Proc. Natl.*
414 *Acad. Sci. U.S.A.* **114,** 13774–13779 (2017).

415

416

Acknowledgments

The authors would like to thank Dr. Timothy Sykes and Dr. Weihong Qi from Functional Genomics Center Zurich (FGCZ) for DNA library preparation, Illumina sequencing and initial data analysis by multi-sample variant calling. Microscopy images were obtained with a Leica Thunder microscope maintained by the Center for Microscopy and Image Analysis at University of Zurich. We would like to thank Prof. R. Elisabeth Sockett (University of Nottingham, UK) for providing *B. bacteriovorus* HD100^{T} and helpful input on our manuscript. Further, we would like to thank Prof. Alex Hall and Dr. Daniel Angst (both ETH Zürich, CH) for the *E. coli* strains from the KEIO collection and pCP20. This study was enabled by FAN (Research Talent Development Fund of the University of Zurich Alumni), the Ernst Göhner Stiftung, as well as the Kurt und Senta Herrmann-Stiftung (all to S.M. and S.G.H.), all of which contributed towards research costs and salary of S.M.. R.K. was funded by a project grant from the Swiss National Science Foundation (no. 310030_212266), S.G.H. was funded by Swiss National Science Foundation Ambizione Fellowship PZ00P3_193401. A CC-BY-NC-ND copyright license is applied to this manuscript.

Author contributions

S.M. and S.G.H. jointly conceived the project and obtained funding with input from R.K. . S.M. and O.Ch.M. conducted the prey evolution experiment and isolated genomic DNA from prey populations for sequencing of ancestor and evolved prey lineages. S.M. and O.Ch.M. isolated single clones of evolved prey lineages and sent them for sequencing. S.M. and O.Ch.M. conducted predation assays with prey of ancestor and evolved lineage populations at the end timepoint (15th evolution cycle). S.M. made predation assays of evolved prey lineage populations at 2nd and 5th evolution cycles as well as evolved single clones (15th evolution cycle). S.L.L. performed predation assays of prey deletion strains with help of S.I. . Data analysis and evaluation of predation assays was done by O.Ch.M., S.L.L., and S.M. (lead). Genome sequence analysis was performed by O.Ch.M. (population), S.G.H. (population, gene mutations), S.L.L. (single clones, OmpF population mutations) and S.M. (population, single clones, all final heatmaps, lead). S.L.L. generated clean deletion strains Δ*ompF,* Δ*waaF,* Δ*envZ,* and Δ*truA.* S.I. and S.G.H. helped S.L.L. to generate Δ*waaB*. S.L.L. took microscopy images of prey ancestor and all evolved prey lineage populations (15th evolution cycle), as well as *E.coli* BW25113, Δ*envZ,* and Δ*truA*, with assistance of S.G.H. . S.L.L. performed image analysis with statistical input by S.M. . S.G.H. advised on predatory bacterial culturing, lab experimentation, prey sequencing, and

molecular genetics aspects. R.K. advised on evolutionary and statistical aspects. S.M., S.G.H. and R.K. wrote the paper with contributions from the other authors. All authors approved of the final version before submission.

Competing interests

The authors declare no competing interests.

Additional information

Extended data is available for this paper at https://doi.org/XXX.

Supplementary information The online version contains supplementary material available at https://doi.org/XXX.

Requests for materials should be addressed to Simona G. Huwiler.

Main figures

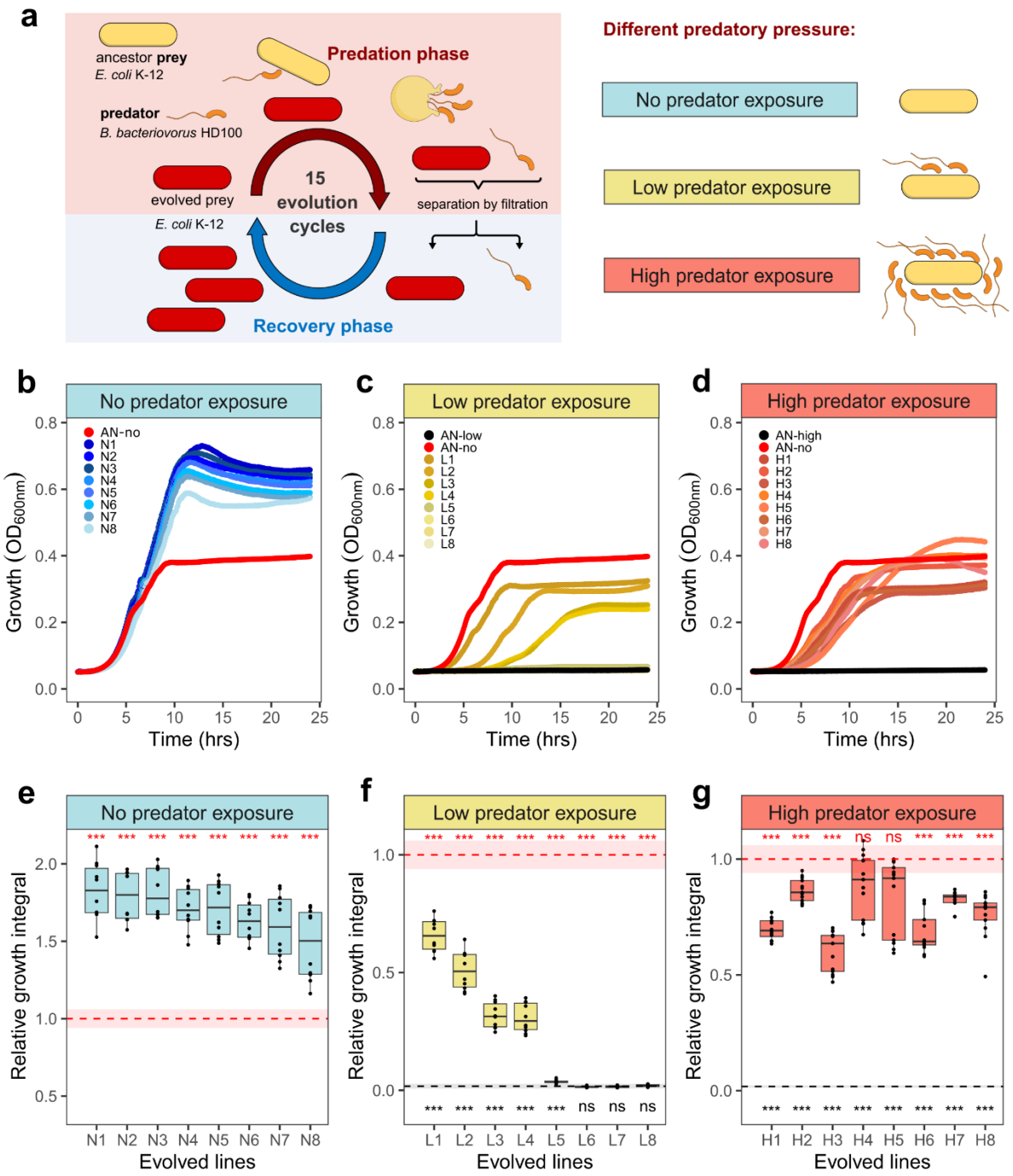

Fig. 1 | Repeated exposure of predator *B. bacteriovorus* HD100 leads to growth of prey *E. coli* K-12 under predation. a, Experimental evolution scheme: eight different prey lineages are exposed repeatedly to different concentration of the predator: no (N1-N8, blue), low (L1-L8, yellow) and high (H1-H8, red) predatory pressure. Each prey evolution cycle is composed of an alternating predation and recovery phase, whereby surviving prey is separated, recovered and re-exposed to predation for 15 cycles. Growth dynamics of evolved prey from 15th cycle: **b-d,** growth curves measured as OD_{600nm}

489 over time of eight independently evolved prey lineages under no (b), low (c) and high (d) predatory
490 pressure when exposed to respective predation conditions where they evolved. They were compared with
491 ancestor under no (AN-no) or specific predatory pressures (AN-low & AN-high). Each point of the
492 growth curves represents average OD_{600nm} at that timepoint across replicates. **e-g,** Relative growth
493 integral of **b-d**, defined as growth integral (area under the curve) divided by the growth integral of
494 ancestor under no predatory pressure. Boxplots represent the median with 25th and 75th percentiles, and
495 whiskers show the 1.5 interquartile range. Red dotted line and shadow indicate the mean and standard
496 deviation range of AN-no. Black dotted lines and shaded areas indicate the mean and standard deviation
497 range of AN under respective predation conditions. The p-value significance levels (two-sided one
498 sample t-tests, $p>0.05$ = ns, $p<0.05$ = *, $p<0.01$ = **, $p<0.001$= ***) in comparison to AN-no is shown
499 by red asterisks and comparison to ancestor under respective predatory pressures are shown by black
500 asterisks. Experiments were repeated independently at least twice, N1-8 (n = 10 replicates), L1-8 (n =
501 10 replicates), H1-8 (n = 13 replicates), AN-no (n = 72 replicates), AN-low (n = 10 replicates) and AN-
502 high (n = 62 replicates).

503

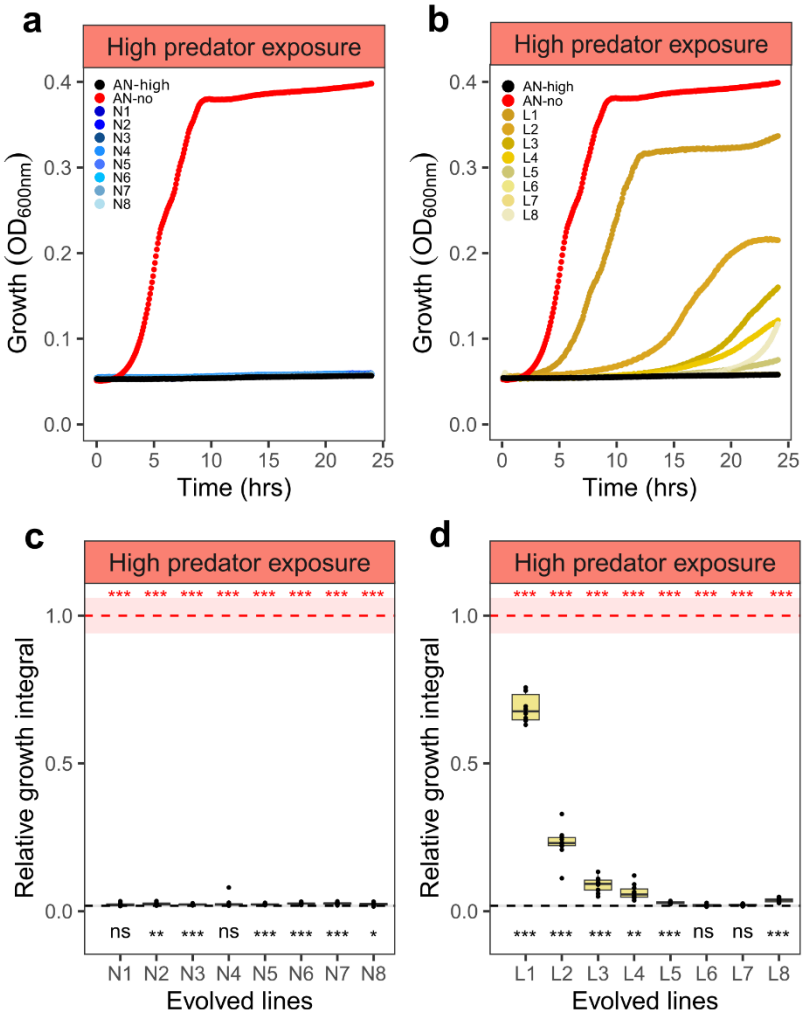

Fig. 2 | Predation resistance evolves only under predation. Growth dynamics of evolved prey from 15th cycle: **a** & **b**, growth curves measured as OD_{600nm} over time of eight independently evolved prey lineages under no (a, N1-8, blue) and low (b, L1-8, yellow) predatory pressure when exposed to high predatory pressure and compared with ancestor population under no (AN-no, red line) and high (AN-high, black line) predatory pressure. Each point of the growth curves represents average OD_{600nm} at that timepoint across replicates. **c** & **d**, Relative growth integral of **a** & **b**, defined as growth integral (area under the curve) divided by the growth integral of AN-no. Boxplots represent the median with 25th and 75th percentiles, and whiskers show the 1.5 interquartile range. Dotted lines and shaded areas indicate the mean and standard deviation range of the ancestor under no (AN-no, red) and high (AN-high, black) predatory pressure. The p-value significance levels (two-sided one sample t-tests, $p>0.05$ = ns, $p<0.05$ = *, $p<0.01$ = **, $p<0.001$= ***) in comparison to AN-no are shown by red asterisks, and to AN-high are shown by black asterisks. Experiments were repeated independently at least twice, N1-8 (n= 10 replicates), L1-8 (n= 10 replicates), AN-no (n= 72 replicates), and AN-high (n= 62 replicates).

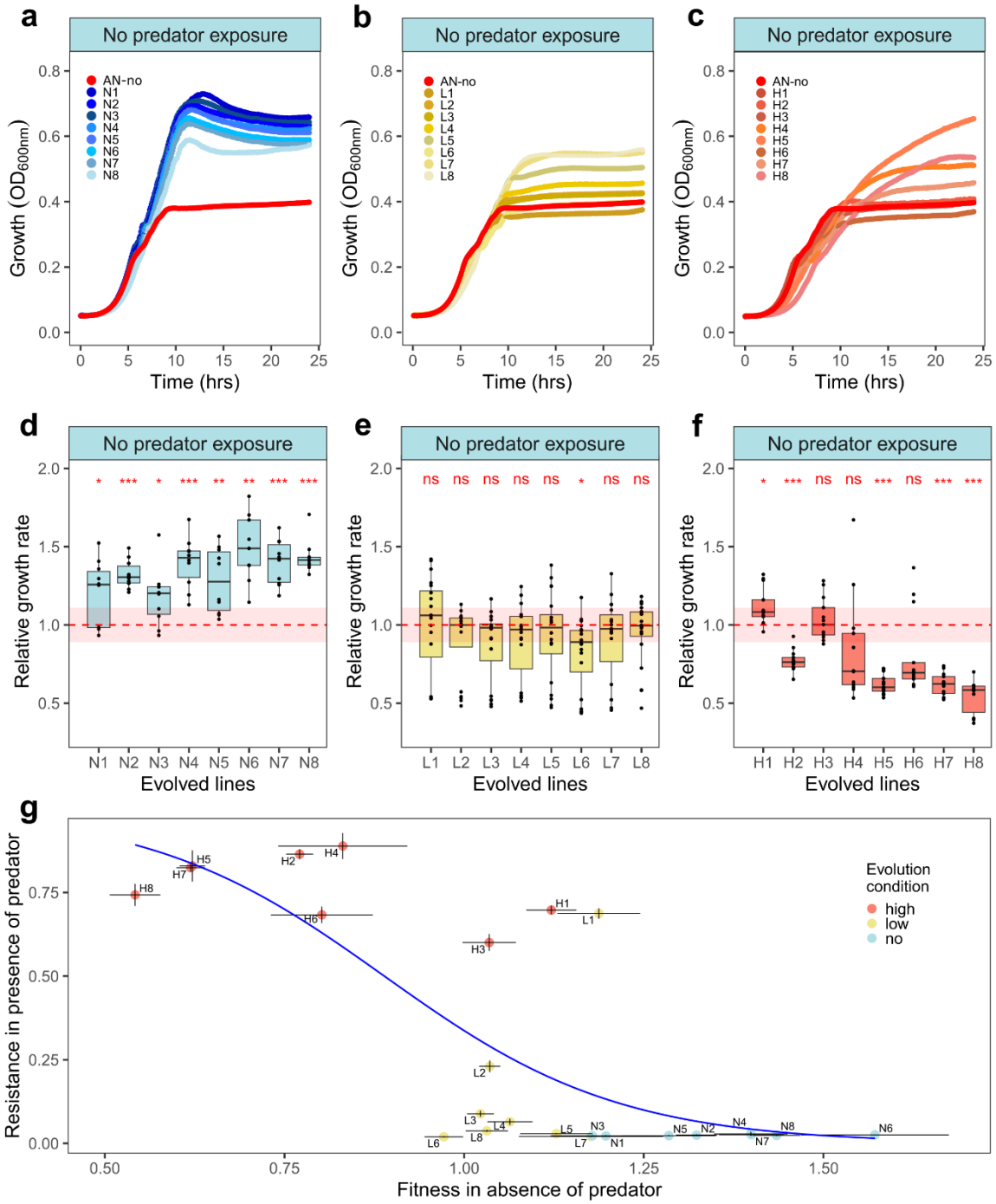

Fig. 3 | Prey resistance to bacterial predator is generally associated with negative fitness consequences. Growth dynamics of evolved prey from 15th cycle: **a-c** growth curves measured as OD600nm over time, of prey lineages evolved under no (**a,** blue), low (**b,** yellow) and high (**c,** salmon) predatory pressure, when exposed to no predatory pressure. Each point of the growth curve represents the average OD600nm at that timepoint across replicates. Panel **a** is identical with Fig. 1a for a complete overview. **d-f,** Relative growth rates of no (**d**), low (**e**), and high (**f**) predatory pressure evolved lines, when exposed to no predatory pressure. Relative growth rate is defined as maximum growth rate divided by the maximum growth rate of the ancestor under no predatory pressure (AN-no).

556 Boxplots represent the median with 25th and 75th percentiles, and whiskers show the 1.5 interquartile
557 range. Red dotted lines and shaded areas indicate the mean and standard deviation range of ancestor
558 under no predatory pressure (AN-no). The p-value significance levels (two-sided one sample t-tests,
559 $p>0.05$ = ns, $p<0.05$ = *, $p<0.01$ = **, $p<0.001$ = ***) in comparison to AN-no are shown by red
560 asterisks. Experiments were repeated independently at least twice, N1-8 (n= 10 replicates), L1-8 (n=
561 20 replicates), H1-8 (n= 13 replicates), AN-no (n= 72 replicates). Three outliers, one each from N6,
562 L4 and L7 were excluded from panels **d & e** for better visualisation but were included in the statistical
563 analysis. **g,** Trade-off between predation resistance and prey fitness. Fitness, quantified as mean
564 relative growth rate under no predatory pressure (**d-f**) versus predator resistance, quantified as mean
565 relative growth integral under high predatory pressure (Fig. 1g & 2c-d). N1-8, L1-8, and H1-8 denotes
566 prey lineages that evolved under no (blue), low (yellow) and high (salmon) predatory pressure
567 respectively. A logistic regression function was fitted as a blue line to correlate the two variables
568 (resistance versus fitness, Wald z-statistics = -2.336, p- value = 0.0195). Black error bars represent the
569 standard error of mean for the respective variables.

570

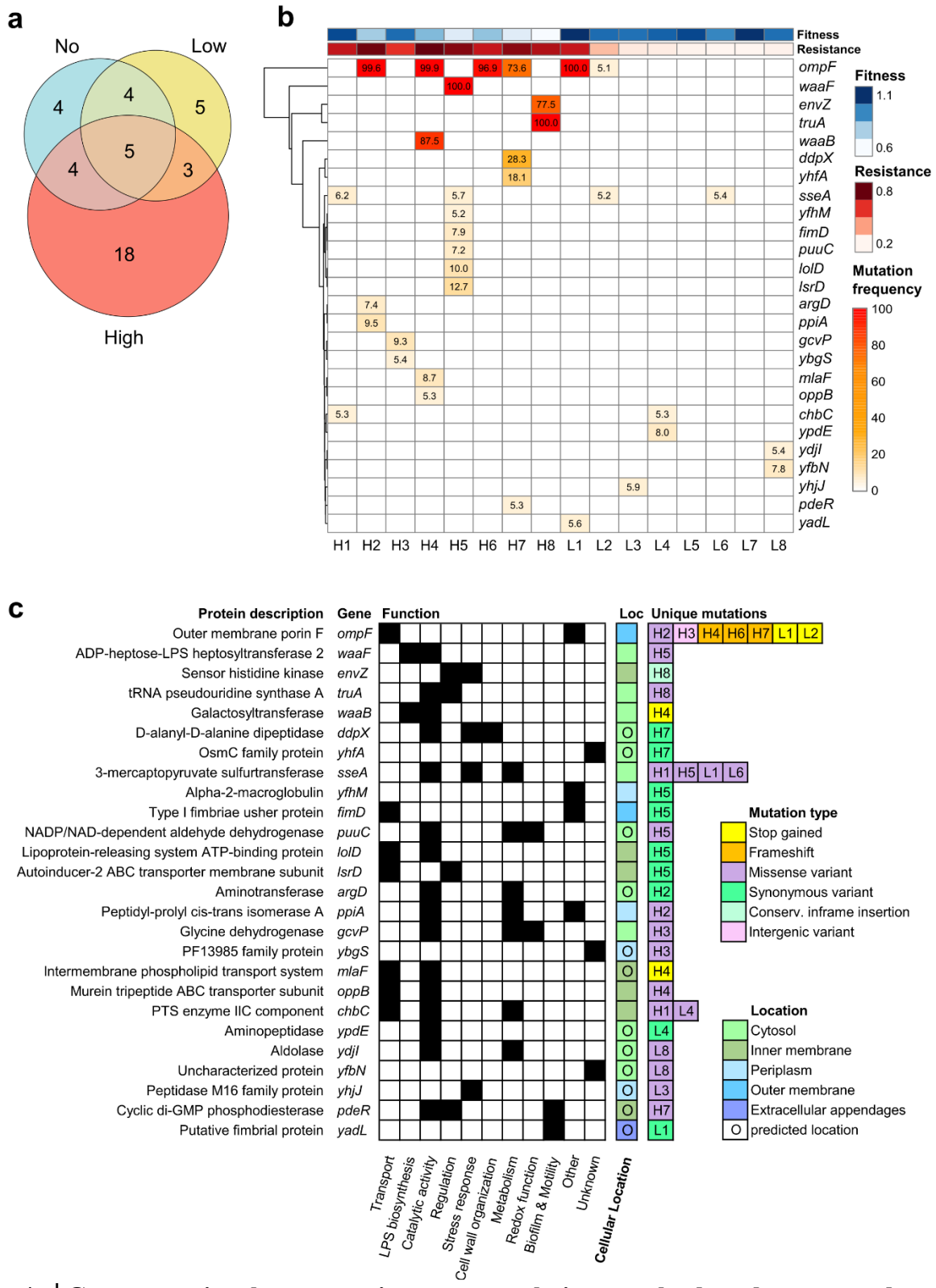

Fig. 4 | Gene mutational patterns in prey populations evolved under repeated predation pressure. Genes mutated in evolved *E. coli* K-12 lineages after the 15th evolution cycle in comparison to the ancestor. **a,** Venn diagram showing the number of mutated *E. coli* genes that reached frequencies higher than 5% within a lineage, grouped according to no, low and high predatory pressure. Not

594 included in this Venn diagram are mutated rRNA and transposase genes, which are listed separately
595 (Extended Data Fig. 7). **b**, Hierarchically clustered heatmap of mutation frequency differences relative
596 to the ancestor of all the genes that exclusively mutated under high (H1-8) and/or low (L1-8) predatory
597 pressure. Heatmaps on top of the panel show fitness (blue) measured as average relative growth rate
598 of lineages under no predatory pressure, and resistance (red) measured as average relative growth
599 integral of lineages under high predatory pressure, according to the data in Fig. 3g. **c**, Overview of
600 mutated genes and mutation types together with a description of the encoded proteins, their functions
601 and cellular location (Loc) for all the genes that exclusively mutated under high and/or low predatory
602 pressure, according to **b**.

603

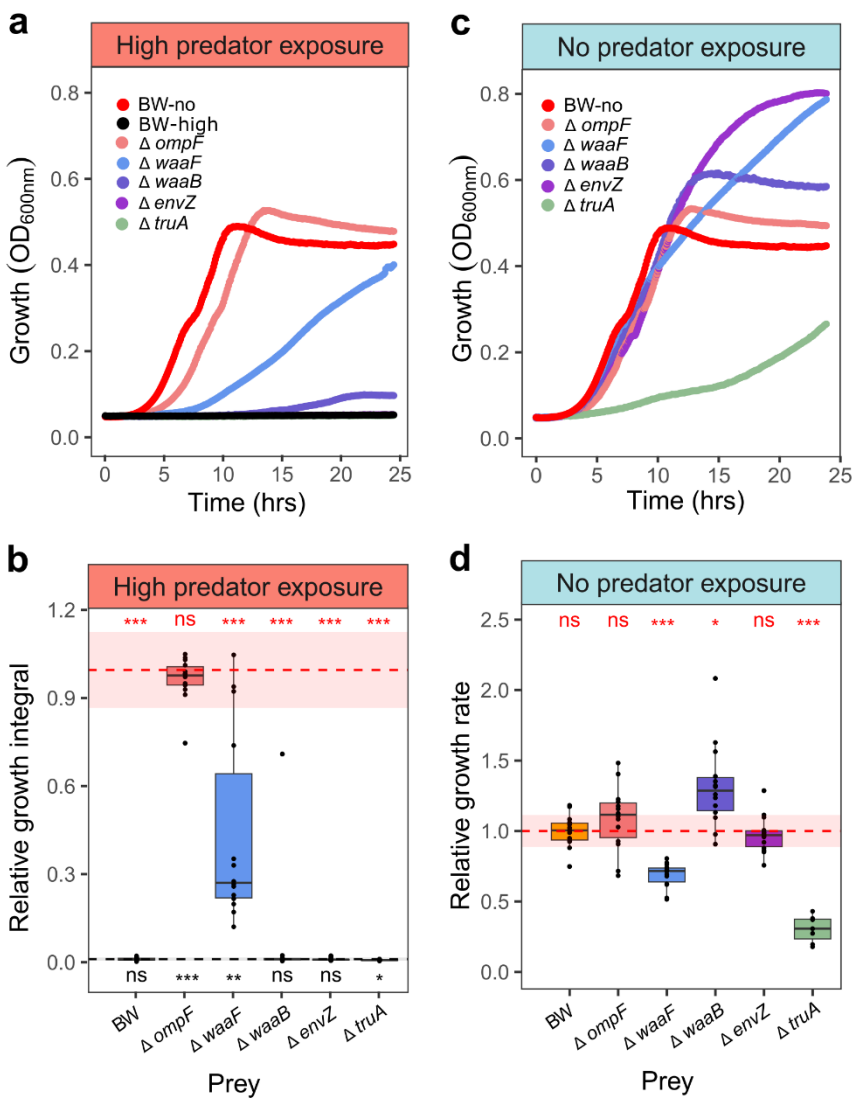

Fig. 5 | OmpF deletion in *E. coli* prey results in high predation resistance. Different *E. coli* clean-deletion mutant strains (Δ*ompF*, Δ*waaF*, Δ*waaB*, Δ*envZ*, Δ*truA*) were generated based on the KEIO library. *E. coli* BW25113 (BW) is the KEIO reference strain. **a+c**, Growth curves measured as OD_{600nm} over time of the different *E. coli* deletion mutants exposed to either high predatory pressure (**a**) or no predators (**c**). Each point of the growth curve represents the average OD_{600nm} per timepoint across replicates. Experiments were independently repeated at least twice. Total replicate numbers for the various strains: Δ*ompF* (n= 14), Δ*waaF* (n= 14), Δ*waaB* (n= 14), Δ*envZ* (n= 14), Δ*truA* (n= 8), BW without predatory pressure (BW-no) (n= 14), and BW with high predatory pressure (BW-high) (n= 15). **b,** Relative growth integrals from **a**. Relative growth integrals are calculated as growth integral (area under the curve) of the clean-deletion mutant with predatory pressure divided by the growth integral of BW-no. **d**, Relative growth rates from **c**. Relative growth rates are calculated as the maximum growth rate of the clean-deletion mutant divided by the maximum growth rate of BW-no .

Boxplots represent the median with 25th and 75th percentiles, and whiskers show the 1.5 interquartile range. Red and black dotted lines and shaded areas indicate the mean and standard deviation range of BW-no and BW-high respectively. The p-value significance levels (two-sided one sample t-tests, $p>0.05$ = ns, $p<0.05$ = *, $p<0.01$ = **, $p<0.001$= ***) in comparison to BW-no (red asterisks), and to BW-high (black asterisks).

636 # Methods

637 ## Growth of bacterial strains

638 In this study, *Escherichia coli* K-12 MG1655 (DSM 18039) as prey and *Bdellovibrio bacteriovorus*
639 HD100^T as predator were used, unless indicated otherwise. *B. bacteriovorus* HD100^T was obtained
640 from the laboratory of Prof. R. E. Sockett at University of Nottingham, UK. *B. bacteriovorus* HD100
641 was cultured and maintained on Ca/HEPES buffer (25 mM HEPES, 2 mM $CaCl_2$, pH 7.6) with late-
642 log *E. coli* K-12 MG1655 at 29°C for generally 24 h at 200 rpm shaking[1]. General revival of
643 *B. bacteriovorus* and determination of plaque forming units (PFU) for enumeration was done according
644 to protocols by Lambert & Sockett[1] and is described in more detail at the end of the Additional Online
645 materials.

646 All *E. coli* strains used are listed in Additional Online Materials Table SOnline1. To validate the
647 genetic effect on predation resistance, markerless single deletion strains Δ*envZ,* Δ*ompF,* Δ*truA,* Δ*waaB,*
648 and Δ*waaF* were generated based on *E.coli* KEIO library strains[2] containing an inserted kanamycin
649 resistance cassette (following section). The different *E. coli* strains were generally grown in YT both
650 (Yeast tryptone, 5 g l^{-1} NaCl, 5 g l^{-1} Bacto yeast extract, 8 g l^{-1} tryptone, pH 7.5) at 37°C with 200 rpm
651 shaking for generally 16 h overnight, and additional appropriate antibiotics as indicated. For ancestor
652 prey, *E. coli* K-12 MG1655 was retrieved from 20% glycerol stocks at -80°C and were streaked on a
653 YT agar plate (YT broth with 10 g l^{-1} agar) and incubated at 37°C for 24 h to obtain single colonies.
654 The overnight cultures from ancestor prey single colonies were used for 24-hr lysates (growth of
655 predator), revival and enumeration of the predator in our experiments.

656

657 ## Generation of markerless deletion strains of *E. coli* KEIO library

658 Markerless single deletion mutants in *E. coli* (Δ*envZ,* Δ*ompF,* Δ*truA,* Δ*waaB,* and Δ*waaF*) were
659 constructed of the respective strain from the KEIO collection (based on *E. coli* BW25113)[2]. To achieve
660 this, the kanamycin resistance cassette (present in the KEIO collection to disrupt the individual genes)
661 was removed to enable predation assays with kanamycin-sensitive *B. bacteriovorus* HD100. The
662 kanamycin cassette was excised via pCP20[3], expressing an FLP-FRT recombinase. To generate
663 electrocompetent cells, and excise the kanamycin cassette, several protocols from the Barrick lab were
664 adapted[4,5]. To prepare electrocompetent cells the desired *E. coli* strain in YT broth with 30 µg/ml

665 kanamycin was incubated for 16 h at 37°C and 200 rpm. The stationary phase culture was used to
666 inoculate at least 10 ml of YT broth with 30 µg/ml kanamycin at optical density with absorbance at
667 600nm (OD_{600nm}) of 0.05 and grown at 37°C and 200 rpm. At an OD_{600nm} of ~ 0.6 the culture was
668 centrifuged for 5 minutes at 6000 x *g* and 4°C, and the supernatant was discarded. The resulting pellet
669 was washed 4 times with 10% ice-cold glycerol of the same volume as the initial inoculation volume.
670 Finally, the pellet was resuspended in 10% glycerol at 100x concentration, and 50 µl aliquots stored at
671 -80°C. These electrocompetent *E. coli* cells were thawed on ice and maximally 100 ng of pCP20 added.
672 After gentle mixing, the sample was transferred into a cooled 0.2-cm cuvette (Bio-Rad), and
673 electroporated at 2.5 kV with a MicroPulser electroporator (Bio-Rad). Then, the sample was
674 resuspended in 500 µl warm SOC medium and incubated for 30 min at 30°C and 120 rpm. The cells
675 were plated on YT agar plates with 100 µg/ml ampicillin and grown at 29°C for at least 16 h. To select
676 for loss of heat-sensitive plasmid pCP20 after recombination, a single colony from a YT agar plate
677 with 100 µg/ml ampicillin was picked to inoculate 5 ml of YT broth, and grown for 16 h at 43°C,
678 shaking at 200 rpm. 50 µl of a 10^{-6} dilution of this stationary phase culture was plated on YT agar
679 without antibiotics for single clones. To screen for successful recombination and loss of plasmid, six
680 colonies were selected and streaked out on YT agar with 30 µg/ml kanamycin, YT agar with 100 µg/ml
681 ampicillin, and YT agar without antibiotics in this order. The YT plates without and with kanamycin
682 were incubated at 37°C, the YT plates with ampicillin at 29°C for at least 16 h. To screen for successful
683 excision of the kanamycin cassette, recombinants with sensitivity to both antibiotics were grown in
684 5 ml of YT broth, incubated for 16 h at 200 rpm and 37°C. Of these cultures, 20% glycerol stocks were
685 made and stored at -80°C. To control correct excision of the kanamycin cassette, PCR was used to
686 assess correct product size (Primers in Additional Online Materials Table SOnline 2). Additionally,
687 correct scar regions were confirmed by sanger sequencing (Microsynth AG, CH).

688

689 **Experimental prey evolution**

690 In the experimental prey evolution, *E. coli* K-12 MG1655 was used as ancestral prey strain and
691 subjected to three different predatory pressures by *B. bacteriovorus* HD100 involving 15 alternate
692 cycles of predation and recovery phase (Fig. 1a). The detailed protocol is described at the end of the
693 Supplementary Online Materials. The predation phase occurred in rich medium (containing ¾ YT, 1/4
694 25 mM HEPES and 2 mM $CaCl_2$) allowing growth of *E. coli* K-12 as well as predation of
695 *B. bacteriovorus* at 200 rpm and 29°C. *E. coli* K-12 prey were subjected to three different predatory

696 conditions: No predatory, low predatory pressure (multiplicity of infection [MOI], ratio of predator
697 (PFU/ml) vs prey cells (CFU/ml), was ~ 2.5) and high predatory pressure (MOI ~10). For each
698 condition eight independent prey lineages were evolved from the *E. coli* K-12 ancestor. After the 24-
699 hr predation phase surviving *E. coli* were separated from *B. bacteriovorus* by filtration to avoid co-
700 evolution. In the subsequent 16-hr recovery phase retrieved *E. coli* from filtration were diluted ~1:100
701 and grown in YT at 200 rpm and 37°C. These overnight cultures were diluted back to an overall initial
702 OD_{600nm} of 0.003 for the next predation phase and evolution cycle.

703

704 **Isolation of prey single clones**

705 Prior to the experiment we made overnight cultures of evolved lineages under high predatory pressure
706 (15th evolution cycle) stored at -80°C, by extracting cell material (containing evolved population) from
707 cryo stocks and inoculating 50 ml YT medium in 250 ml Erlenmeyer flasks, incubated at 37°C,
708 200 rpm for 16 h. We harvested prey cells from 10ml of these overnight cultures by centrifugation at
709 5311 x *g* for 3 min and subsequently washed them in 10 ml of Ca-HEPES. Then prey cells were
710 resuspended in 6 ml of Ca-HEPES and adjusted to $OD_{600nm} = 3.0$, then we diluted the cultures to 10^{-6}
711 and plated 100 µl on YT agar plates and incubated them at 37°C for 24 h. We randomly selected 6
712 single colonies from each evolved lineage and overnight cultures were made with these single colonies
713 in 10 ml YT medium in 50 ml Falcon tubes incubated at 37°C, 200 rpm for 16 h. From this culture we
714 prepared 20% glycerol stocks and stored them at -80°C. Prior to experiments, we made overnight
715 cultures of the single colonies from cryo stocks, alongside their respective evolved lineage population
716 and ancestor in 50 ml YT medium in 250 ml Erlenmeyer flasks, incubated at 37°C, 200 rpm for 16
717 hours. These single clone cultures were used for predation assays and genome sequencing.

718

719 **Predation assay**

720 To evaluate predation resistance and growth dynamics of different prey, predation assays were
721 performed. Different *E. coli* prey strains were assessed: *E. coli* K-12 MG1655 population lineages
722 evolved under high (H1-8), low (L1-8) and no (N1-8) predatory pressure at the end 15th evolution cycle
723 (after recovery phase) were compared with ancestor *E. coli* K-12 MG1655. At first, we exposed prey

724 lineages that evolved under a particular predatory pressure to that pressure. We then focussed on
725 exposing evolved lines to the high predatory pressure condition.

726 To investigate the temporal aspect of evolution, we performed predation assays of prey lineages
727 evolved under high predatory pressure (H1-H8) at the end of the 2nd and 5th evolution cycle and
728 compared them to the 15th cycle, when exposed to high predatory pressure. To test for cross resistance,
729 we assessed the performance of prey that evolved under no or low predator by exposing them to high
730 predatory pressure. The predation assays at the population level featured 5 replicates per prey-predator
731 combination and were repeated on two separate days.

732 To assess effects of specific prey genes on predation resistance, predation assay was conducted with
733 markerless single gene deletion mutants (Δ*envZ,* Δ*ompF,* Δ*truA,* Δ*waaB,* and Δ*waaF* based on *E. coli*
734 BW25113 (reference strain from KEIO library[2]). These strains were exposed to high and no predatory
735 pressure conditions.

736 Prior to the predation assay, respective evolved prey lineages or prey strains (evolved lineages,
737 population- or single clone-based, single gene deletion, and KEIO reference strain) were grown from
738 cryo stocks by inoculation in 50 ml YT broth and incubation at 37°C and 200 rpm for 16 h.
739 Additionally, an overnight culture of ancestor prey was prepared from a single colony, at same growth
740 conditions. The eight independently evolved prey lineages under each predatory pressure were assessed
741 in parallel alongside ancestor prey. 10-ml prey overnight cultures were centrifuged at 5311 x *g* for 3
742 min and subsequently washed with 10 ml of Ca-HEPES buffer. Then prey cells were resuspended in
743 6 ml of Ca-HEPES buffer and adjusted to OD_{600nm} = 0.03. A 24-hr predator lysate was filtered through
744 a 0.8-µm syringe filter (Whatman® Puradisc FP 30, Cellulose Acetate, sterile, WHA10462240). For
745 the predation assays, the same cultivation media was used as for the experimental evolution predation
746 phase, comprising 15 ml of YT broth, 5 ml of 25 mM HEPES and 2 mM $CaCl_2$ overall. We set up the
747 predation assay in 96-well plates, in a total volume of 150 µl. Initially 119 µl of cultivation media was
748 preset, and different volumes of the filtered predator lysate were added to the assay: 0 µl (no predator
749 exposure), 4 µl (low predator exposure) or 16 µl (high predator exposure), depending on the evolved
750 prey lineages and predatory pressure tested. Then we added 15 µl of the respective prey solution
751 (OD_{600nm} = 0.03 in Ca-HEPES). Then we adjusted the final volume in reaction wells to 150 µl by
752 adding Ca-HEPES (as proxy for predator lysate and prey resuspension), resulting in a final
753 concentration of prey of OD_{600nm} = 0.003. We used the same ratio of prey and predator as in the

754 predation phase of the prey evolution experiment. The plate was incubated in a plate reader (Tecan
755 Infinite 200 Pro) at 29°C for 24 h. OD_{600nm} of the reaction wells was measured with 10 flashes every
756 5 minutes after shaking at 6-mm amplitude for 120 secs.

757 We used OD_{600nm} as proxy for the biomass of prey cells, as the predator cells only contribute to a very
758 minor fraction to OD_{600nm} based on the small size. The kinetic measurement of OD_{600nm} over 24 h, was
759 analysed using an interactive platform for analysis of microbial growth data
760 (https://statu.shinyapps.io/ExploreMicrobialGrowth/, version 2016.01.12) designed by Adin Ross-
761 Gillespie at University of Zurich. We used Spline function to fit the kinetic growth data to extract the
762 integral (area under the curve) and maximal growth increase rate. For the predation assays in cultivation
763 media, we derived relative growth integral and growth rate of evolved prey lineages in comparison to
764 the ancestor prey. For this we divided the growth integral or growth rate of evolved lineages under all
765 predator conditions by that of ancestor when exposed to no predator, that is baseline. Values > 1 or <
766 1, indicate that evolved lineages perform better or worse than baseline.

767

768 **Cell shape analysis by phase-contrast microscopy**

769 *E. coli* K-12 lineages evolved under low, no, and high predatory pressure at the end of experimental
770 evolution (after the 15th evolution cycle), *E. coli* K-12 MG1655 (ancestor), as well as *E. coli* K-12
771 BW25113, Δ*envZ* and Δ*truA* were regrown from cryo stocks in YT broth at 37°C and 200 rpm shaking
772 overnight. From each culture 10 µl was applied onto a 1% agarose in Ca/HEPES buffer pad on a clean
773 microscope slide for phase-contrast microscopy. Imaging was performed using a Leica DMi8 inverted
774 microscope equipped with a 100x objective (HC PL APO 1.40 oil PH3), a Leica monochrome
775 fluorescence DFC9000 gTC Camera System, and Leica Application Suite X Software Version
776 3.7.6.25997 (Leica microsystems). Exposure time was 100 ms with illumination intensity of 140. For
777 each evolved lineage and ancestor strain *E. coli* K-12 MG1655 a minimum of 15 images were
778 collected. For shape analysis of the evolved cells, software Fjij/ImageJ (Version 2.90/1.53t, Java
779 1.8.0322, 64-bit)[6,7] was used with the Plugin MicrobeJ (Version 5.13o (16) – beta)[8]. Area and length
780 restrictions were set to 0.5-3 p^2, width to 0.5-2 p^2. After initial shape detection, masks were manually
781 adjusted to observed cell size and a minimum of 300 cells per lineage/strain were analysed.

782

783 **Statistical analyses**

784 We used general linear models for statistical analysis in R 4.2.3[9,10]. To assess whether relative growth
785 integral and relative growth rate vary in response to predatory pressure we used analysis of variance
786 (ANOVA) models (Fig. 1e-g, Fig. 2 c,d & Fig. 3d-f). We further used two-sided one-sample *t*-tests to
787 test for significant differences in relative growth integral or growth rate between evolved prey lineages
788 and that of ancestor when exposed to either no, low or high predatory pressure (i.e. being different
789 from mean relative growth integral or growth rate of ancestor, Fig. 1e-g & Fig. 2c-d & Fig. 3d-f & Fig.
790 5b,d & Extended Data Fig. 2d-f, j-l). Reported p-values for *t*-tests were adjusted for multiple testing
791 using the Holm method. We used a logistic regression model to test for a negative association (tradeoff)
792 between mean relative growth integral and mean relative growth rate (Fig. 3g). A detailed statistical
793 output of the data of this article is available in an Additional Online Material table.

794

795 **Genome sequencing and analysis of evolved prey population lineages**

796 We sequenced the genome of the 24 prey lineages (i.e. population) that evolved under no, low and high
797 predatory pressure condition (8 each) after the 15th evolution cycle, at the population level and
798 compared it with the ancestor prey genome. Overnight cultures were grown in YT broth (200 rpm at
799 37°C) from cryo stocks of evolved prey lineages from the 15th recovery phase at the end of
800 experimental evolution and separately from a single colony of the ancestor prey. From these cultures
801 we extracted genomic DNA using GenElute^{TM} Bacterial Genomic DNA Kit (Sigma, NA2110). The
802 concentration of genomic DNA varied between 83.77 to 205. 407 ng/µl, which was sufficient for
803 standard library preparation. The samples were then transferred to the Functional Genomic Center
804 Zurich (FGCZ, Switzerland) for sequencing and base variant calling of the sequencing data of evolved
805 lineages against the ancestor. For library preparation the TruSeq DNA Nano Sample Prep Kit v2
806 (Illumina, Inc, California, USA) was used in the succeeding steps. DNA samples (100ng) were
807 sonicated with the Covaris using settings specific to the fragment size of 350 bp. The fragmented DNA
808 samples were size- selected using AMpure beads, end-repaired and adenylated. TruSeq adapters
809 containing Unique Dual Indices (UDI) for multiplexing were ligated to the size-selected DNA samples.
810 Fragments containing TruSeq adapters on both ends were selectively enriched by PCR. The quality
811 and quantity of the enriched libraries were validated using TapeStation (Agilent, Waldbronn,
812 Germany). An average fragment size of approximately 500 bp was achieved. The libraries were

813 normalized to 10 nM in Tris-Cl 10 mM, pH 8.5 with 0.1% Tween 20. For sequencing and cluster
814 generation the Novaseq 6000 (Illumina, Inc, California, USA) was used according to standard protocol.
815 Sequencing were paired end at 2 X150 bp. Technical quality of Illumina paired-end (PE) reads was
816 evaluated using FastQC (v0.11.9) and FastQScreen (v0.14.1). Raw reads were pre-processed using
817 fastp (v0.20.0) with the following parameter: hard trimming of 10 nucleotide (nt) and 1 nt at 5' and 3
818 ends, respectively; quality trimming of both ends using a sliding window of 4 nt and mean quality of
819 20; trimmed reads shorter than 18 nt, and trimmed reads with mean read quality lower than 20 were
820 filtered out. Pre-processed PE reads were aligned to the reference genome (*E. coli* K-12 MG1655 refseq
821 GCF_000005845.2) using bwa (v0.7.17) with the "mem" algorithm. PCR duplicates were marked
822 using Picard (v2.22.8, MarkDuplicates). Mapping results were quality controlled using SAMStat
823 (v1.5.1), Qualimap (v2.2.1), and Picard (v2.22.8, CollectGcBiasMetrics). Multi-sample variant calling
824 was performed using freebayes (V1.3.2) with frequency cutoffs of 5% and 1%, respectively. Only
825 unique reads in primary alignments with alignment quality 30 and above, and bases with quality 20
826 and above, were counted for variant analysis. Sites with multiple alternative alleles were split into
827 multiple rows using bcftools. Variant annotation was performed using snpEff (v4.3) against reference
828 gene models (NCBI, reference genome: ASM584v2, refseq: GCF_000005845.2). Called variants were
829 filtered against the ancestor strain using a customized Perl script. Markers were retained, where all
830 counted reads contain only the reference alleles in the ancestor strain. Per sample variant frequencies
831 were then calculated for these markers using the customized Perl script. The resulting excel file from
832 population variant calling was used for further analysis and representation by hierarchically clustered
833 heatmaps on absolute mutation frequencies and their differences compared to the ancestor strain.
834 Heatmaps were generated in R with Pheatmap[11]. We focused on gene mutations with a frequency more
835 than 5%. If a particular gene had multiple mutation effects, we selected the mutation with the highest
836 frequency. Mutation counts were added to a gene only if the mutation was located within the coding
837 region of a specific gene (direct effects). This excludes downstream effects on adjacent genes.
838 Mutations lying in intergenic regions were ignored due to their ambiguous impact on surrounding
839 genes. An exception was made for the mutation located in the intergenic region between *asnS* and
840 *ompF*. Since it is located 143 bp upstream the *ompF* transcription start site various *ompF* regulators
841 bind adjacent to this locus and is likely to influence *ompF* transcription. The mutations in *ompF* were
842 analysed in detail and the OmpF amino acid sequence with changes in the different prey lineages was
843 constructed in Excel (Microsoft Corporation, 2018) and compared with the ancestor strain. Uniquely
844 mutated genes (without transposases and rRNA genes) of all genomes of prey lineages at the respective
845 predatory pressure were plotted using R package VennDiagram[12].

846

847 **Genome sequencing and variant calling for prey single clones**

848 48 cultures were prepared from six single prey clones each of all eight prey lineages evolved under
849 high predatory pressure (H1-H8) at the end of the 15th evolution cycle. Overnight cultures of these
850 single clones from lineages evolved under high-predatory pressure were inoculated from cryo stocks
851 into 10 ml YT medium in 50 ml Falcon tubes, and incubated at 37°C, 200 rpm for 16 h. We harvested
852 prey cells equivalent of OD_{600nm} = 10.0 from these cultures by centrifugation at 5000 *g* for 5 min, the
853 cells were then washed (5000 g for 5 minutes) in 1 ml Phosphate buffered saline (Gibco) and
854 resuspended into 0.5ml DNA/RNA shield buffer (Zymo Research). This mixture was sent to
855 MicrobesNG (UK, https://microbesng.com, Birmingham, UK), for DNA extraction, sequencing and
856 base variant calling against reference genome *E. coli* K-12 MG1655.

857 DNA was extracted by lysing 4-5 µl cell suspension with 120 µL of TE buffer containing lysozyme
858 (MPBio, USA), metapolyzyme (Sigma Aldrich, USA) and RNase A (ITW Reagents, Spain), and
859 incubated for 25 min at 37°C. Proteinase K (VWR Chemicals, Ohio, USA) (final concentration
860 0.1mg/mL) and SDS (Sigma-Aldrich, Missouri, USA) (final concentration 0.5% v/v) are added and
861 incubated for 5 min at 65°C. Genomic DNA was purified using an equal volume of SPRI beads and
862 resuspended in EB buffer (10mM Tris-HCl, pH 8.0). The DNA was quantified with the Quant-iT
863 dsDNA HS (ThermoFisher Scientific) assay in an Eppendorf AF2200 plate reader (Eppendorf UK Ltd,
864 United Kingdom) and diluted as appropriate. Genomic DNA libraries are prepared using the Nextera
865 XT Library Prep Kit (Illumina, San Diego, USA) following the manufacturer's protocol with the
866 following modifications: input DNA is increased 2-fold, and PCR elongation time is increased to
867 45 sec. DNA quantification and library preparation are carried out on a Hamilton Microlab STAR
868 automated liquid handling system (Hamilton Bonaduz AG, Switzerland). Libraries are sequenced on
869 an lllumina NovaSeq 6000 (Illumina, San Diego, USA) using a 250 bp paired end protocol. For projects
870 predating April, 2020, libraries were sequenced on an Illumina HiSeq 2500 using a 250 bp paired-end
871 protocol (Illumina, San Diego, USA). Reads are adapter trimmed using Trimmomatic version 0.30 [13]
872 with a sliding window quality cutoff of Q15. De novo assembly is performed on samples using SPAdes
873 version 3.7 [14], and contigs are annotated using Prokka version 1.11 [15]. Reads were aligned to the
874 reference using BWA mem v0.7.17 [16] and are then processed using SAMtools v1.9 [17]. Variants were
875 called using VarScan v2.4.0 [18] with two thresholds, sensitive and specific, where the variant allele
876 frequency is greater than 10% respectively. The effects of the variants are predicted and annotated

using SnpEff v4.3 [19]. The base variant calling was performed using the criteria of a sequence coverage of at least 3x and a frequency of at least 10% to generate a table reporting on the differences to the reference genome (NCBI, refseq: GCF_000005845.2). The resulting Microsoft Excel table obtained from Microbes NG was used to combine it with the population sequencing data based on the nucleotide position. Gene annotations were obtained from both population and clone sequencing data, with frequency more than 5%.

Data availability. The raw data (OD_{600nm} measurements over time, microscopy images and raw data on width and length, R code used for analysis) used to generate the findings of this project have been deposited in the figshare repository (doi: XXX). The sequencing data for this study has been deposited in the European Nucleotide Archive (ENA) at EMBL-EBI under accession number PRJEB78919 (https://www.ebi.ac.uk/ena/browser/view/PRJEB78919).

References (Methods):

1. Lambert, C. & Sockett, R. E. Laboratory maintenance of Bdellovibrio. *Curr Protoc Microbiol* Chapter **7,** Unit 7B.2 (2008).

2. Baba, T., Ara, T., Hasegawa, M., Takai, Y., Okumura, Y., Baba, M., Datsenko, K. A., Tomita, M., Wanner, B. L. & Mori, H. Construction of *Escherichia coli* K-12 in-frame, single-gene knockout mutants: the Keio collection. *Molecular Systems Biology* **2,** 2006.0008 (2006).

3. Datsenko, K. A. & Wanner, B. L. One-step inactivation of chromosomal genes in *Escherichia coli* K-12 using PCR products. *Proc. Natl. Acad. Sci. U.S.A.* **97,** 6640–6645 (2000).

4. Barrick Lab. Barrick Lab :: ProtocolsElectrocompetentCells. at <https://barricklab.org/twiki/bin/view/Lab/ProtocolsElectrocompetentCells>

5. Barrick Lab. Barrick Lab :: ProcedureFLPFRTRecombination. at <https://barricklab.org/twiki/bin/view/Lab/ProcedureFLPFRTRecombination>

903 6. Schindelin, J., Arganda-Carreras, I., Frise, E., Kaynig, V., Longair, M., Pietzsch, T., Preibisch,
904 S., Rueden, C., Saalfeld, S., Schmid, B., Tinevez, J.-Y., White, D. J., Hartenstein, V., Eliceiri,
905 K., Tomancak, P. & Cardona, A. Fiji: an open-source platform for biological-image analysis.
906 *Nat Methods* **9,** 676–682 (2012).

907 7. Rueden, C. T., Schindelin, J., Hiner, M. C., DeZonia, B. E., Walter, A. E., Arena, E. T. &
908 Eliceiri, K. W. ImageJ2: ImageJ for the next generation of scientific image data. *BMC*
909 *Bioinformatics* **18,** 529 (2017).

910 8. Ducret, A., Quardokus, E. M. & Brun, Y. V. MicrobeJ, a tool for high throughput bacterial cell
911 detection and quantitative analysis. *Nat Microbiol* **1,** 16077 (2016).

912 9. R Core Team. *R: A language and environment for statistical computing.* (Vienna, Austria,
913 2021). at <https://www.R-project.org/>

914 10. Wickham, H., Averick, M., Bryan, J., Chang, W., McGowan, L., François, R., Grolemund, G.,
915 Hayes, A., Henry, L., Hester, J., Kuhn, M., Pedersen, T., Miller, E., Bache, S., Müller, K.,
916 Ooms, J., Robinson, D., Seidel, D., Spinu, V., Takahashi, K., Vaughan, D., Wilke, C., Woo, K.
917 & Yutani, H. Welcome to the Tidyverse. *JOSS* **4,** 1686 (2019).

918 11. Kolde, R. *Pheatmap: pretty heatmaps.* (R Package Version 1.0.10., 2019). at <https://CRAN.R-
919 project.org/package=pheatmap>

920 12. Chen, H. *VennDiagram: Generate High-Resolution Venn and Euler Plots*. (R package version
921 1.7.3, 2022). at <https://CRAN.R-project.org/package=VennDiagram>

922 13. Bolger, A. M., Lohse, M. & Usadel, B. Trimmomatic: a flexible trimmer for Illumina sequence
923 data. *Bioinformatics* **30,** 2114–2120 (2014).

924 14. Bankevich, A., Nurk, S., Antipov, D., Gurevich, A. A., Dvorkin, M., Kulikov, A. S., Lesin, V.
925 M., Nikolenko, S. I., Pham, S., Prjibelski, A. D., Pyshkin, A. V., Sirotkin, A. V., Vyahhi, N.,
926 Tesler, G., Alekseyev, M. A. & Pevzner, P. A. SPAdes: A New Genome Assembly Algorithm
927 and Its Applications to Single-Cell Sequencing. *Journal of Computational Biology* **19,** 455–477
928 (2012).

929 15. Seemann, T. Prokka: rapid prokaryotic genome annotation. *Bioinformatics* **30,** 2068–2069
930 (2014).

931 16. Li, H. Aligning sequence reads, clone sequences and assembly contigs with BWA-MEM.
932 Preprint at http://arxiv.org/abs/1303.3997 (2013)

933 17. Danecek, P., Bonfield, J. K., Liddle, J., Marshall, J., Ohan, V., Pollard, M. O., Whitwham, A.,
934 Keane, T., McCarthy, S. A., Davies, R. M. & Li, H. Twelve years of SAMtools and BCFtools.
935 *GigaScience* **10,** giab008 (2021).

936 18. Koboldt, D. C., Chen, K., Wylie, T., Larson, D. E., McLellan, M. D., Mardis, E. R., Weinstock,
937 G. M., Wilson, R. K. & Ding, L. VarScan: variant detection in massively parallel sequencing of
938 individual and pooled samples. *Bioinformatics* **25,** 2283–2285 (2009).

939 19. Cingolani, P., Platts, A., Wang, L. L., Coon, M., Nguyen, T., Wang, L., Land, S. J., Lu, X. &
940 Ruden, D. M. A program for annotating and predicting the effects of single nucleotide
941 polymorphisms, SnpEff: SNPs in the genome of *Drosophila melanogaster* strain w ^{1118} ; iso-2;
942 iso-3. *Fly* **6,** 80–92 (2012).